



OPEN ACCESS

EDITED BY

Ahmed A. Abdala,
Texas A&M University at Qatar, Qatar

REVIEWED BY

Payam Hayati,
Iran University of Science and
Technology, Iran
Ratiram Gomaji Chaudhary,
Seth Kesarimal Porwal College of Arts and
Science and Commerce, India

*CORRESPONDENCE

Ziyad Shihab Ahmed AL-Sarraj,
✉ Ziyadshihab.ahmedalsarraj@gmail.com
✉ ziad.shihab@au.edu.iq

RECEIVED 01 February 2023

ACCEPTED 26 May 2023

PUBLISHED 13 June 2023

CITATION

Qubais Saeed B, Waleed I,
Chlib Alkaaby HH, Farhan Jawad S,
Altimari US, Ahmed AL-Sarraj ZS,
Shbeeb RT, Hadrawi SK, Suliman M and
Alshahrani MY (2023), Synthesis of novel
Fe₃O₄ nanostructures surrounded by Ti-
MOF nanostructures as bioactive and
efficient catalysts in three-component
synthesis of new pyrazole derivatives.
Front. Mater. 10:1156702.
doi: 10.3389/fmats.2023.1156702

COPYRIGHT

© 2023 Qubais Saeed, Waleed, Chlib
Alkaaby, Farhan Jawad, Altimari, Ahmed
AL-Sarraj, Shbeeb, Hadrawi, Suliman and
Alshahrani. This is an open-access article
distributed under the terms of the
[Creative Commons Attribution License
\(CC BY\)](https://creativecommons.org/licenses/by/4.0/). The use, distribution or
reproduction in other forums is
permitted, provided the original author(s)
and the copyright owner(s) are credited
and that the original publication in this
journal is cited, in accordance with
accepted academic practice. No use,
distribution or reproduction is permitted
which does not comply with these terms.

Synthesis of novel Fe₃O₄ nanostructures surrounded by Ti-MOF nanostructures as bioactive and efficient catalysts in three-component synthesis of new pyrazole derivatives

Balsam Qubais Saeed¹, Ibrahim Waleed²,
Hussein Humedy Chlib Alkaaby³, Sabrean Farhan Jawad⁴,
Usama S. Altimari⁵, Ziyad Shihab Ahmed AL-Sarraj^{6*},
Ruwaida T. Shbeeb⁷, Salema K. Hadrawi⁸, Muath Suliman⁹ and
Mohammad Y. Alshahrani⁹

¹Department of Clinical Sciences, College of Medicine, University of Sharjah, Sharjah, United Arab Emirates, ²Medical Technical College, Al-Farahidi University, Baghdad, Iraq, ³Al-Manara College for Medical Sciences, Maysan, Iraq, ⁴Pharmacy Department, Al-Mustaqbal University College, Babylon, Iraq, ⁵Department of Medical Engineering, Al-Nisour University College, Baghdad, Iraq, ⁶Department of Biomedical Engineering, Ashur University College, Baghdad, Iraq, ⁷Department of Medical Engineering, Al-Hadi University College, Baghdad, Iraq, ⁸Refrigeration and Air-Conditioning Technical Engineering Department, College of Technical Engineering, The Islamic University, Najaf, Iraq, ⁹Department of Clinical Laboratory Sciences, College of Applied Medical Sciences, King Khalid University, Abha, Saudi Arabia

Synthesis and reporting of new nanoparticles with diverse properties is important in chemistry. A one-step, rapid and controllable synthesis of the new Fe₃O₄ surrounded in Ti-MOF nanostructures was carried out with microwave technology. After identifying and confirming the structure, Fe₃O₄ surrounded in Ti-MOF nanostructures was used as a suitable catalyst with high thermal resistance and recyclable in a three-component reaction of phenylhydrazine, malononitrile and aldehyde to synthesis novel pyrazole derivatives. Continuing investigations on Fe₃O₄ surrounded in Ti-MOF nanostructures, its antimicrobial properties were tested on Gram-positive bacterial species, Gram-negative bacterial species and fungi bacterial. Identification of Fe₃O₄ surrounded in Ti-MOF nanostructures with morphology and size distribution technique (SEM), surface area technique (BET), Infrared spectroscopy (FT-IR), Energy-Dispersive X-ray spectroscopy (EDX/EDX mapping), and Vibrating Sample Magnetometer (VSM) were performed. Synthesized pyrazole derivatives with Fe₃O₄ surrounded in Ti-MOF nanostructures than previously reported methods have less synthesis time and high efficiency. In antimicrobial properties high effects were observed based on MIC, MBC, and MFC values.

KEYWORDS

Fe₃O₄/Ti-MOF nanostructure, magnetic nanocatalyst, pyrazole, Gram-positive bacterial species, Gram-negative bacterial species

1 Introduction

Recently, there have been many reports on the capabilities and applications of different nanostructures. Catalyst ability (Farsi, Mohammadi, and Saghanezhad, 2021), photocatalyst ability (Karimipour et al, 2021; Eshghi et al, 2023), and biological activity such as antimicrobial and antioxidant activity (Aghaei et al, 2022; Akbari et al, 2022) are an example of them. Metal-organic frameworks (MOFs) are nanocompounds that have attracted the attention of scientists recently due to their unique capabilities (Karimi et al, 2021). One of the most important reported uses of these compounds is their energy applications (Sharafi-Badr, Hayati, and Mahmoudi, 2022). Due to the widespread use of nanostructures such as MOFs, efficient synthesis methods of these samples are an essential issue. Investigations show that choosing the method of synthesizing MOF nanostructures, developing new nanostructures, and improving their surface properties is an essential and profound challenge (Zhou et al, 2022), and the properties of the final product are affected by the physical properties and the nature of the structure (Asghar, Iqbal, and Noor, 2020). One of the most effective methods for synthesizing these nanostructures is the microwave technique. The use of microwave paths in synthesizing MOF nanostructures has improved the physicochemical properties of these nanostructures. Crystallinity, thermal stability, and particle size distribution are among these properties (Abd El Salam

and Sharara, 2019). The synthesis of nanostructures in a high specific level of the product and short time are other features of this efficient method (Abdi et al, 2022). A magnetic core-shell structure of MOF magnets can be synthesized. Easy recycling in use as a catalyst for the synthesis of heterocyclic compounds is a distinctive property of core-shell magnetic nanostructures.

Pyrazole derivatives are heterocyclic compounds that have shown broad pharmacological and pharmacological properties. This kind of heterocyclic compound has been used alone or together with various other structures such as antifungal agents (Bendaha et al, 2011), antiviral agents (El-Sabbagh et al, 2009), antidepressant agents (Abdel-Aziz, Abu-Rahma, and Hassan, 2009), antimicrobial agents (Gouda et al, 2010), and sectional agonists for nicotinic acid receptors (Van Herk et al, 2003), p38 kinase inhibitors (Graneto et al, 2007), and CDK inhibitors (Kryštof et al, 2006).

Synthetic derivatives of pyrazole are often widely used in developing anticancer agents (Kumar, Saini, et al, 2013a). Furthermore, natural products containing pyrazole have shown medicinal properties. As shown in Figure 1, some pyrazole derivatives such as 4-methylpyrazole-3(5)-carboxylic acid, pyrazophorin, and pyrazophorin B that are isolated from natural products with medicinal properties have been shown (Kumar, Kaur, et al, 2013b).

The experiment indicates that, in the pyrazole ring, the presence of cyano, aryl, or amino groups as specific substituents has an effective role in observing biological and bioactive effects (Mitchell et al, 2015). Therefore, it can be said that, from the

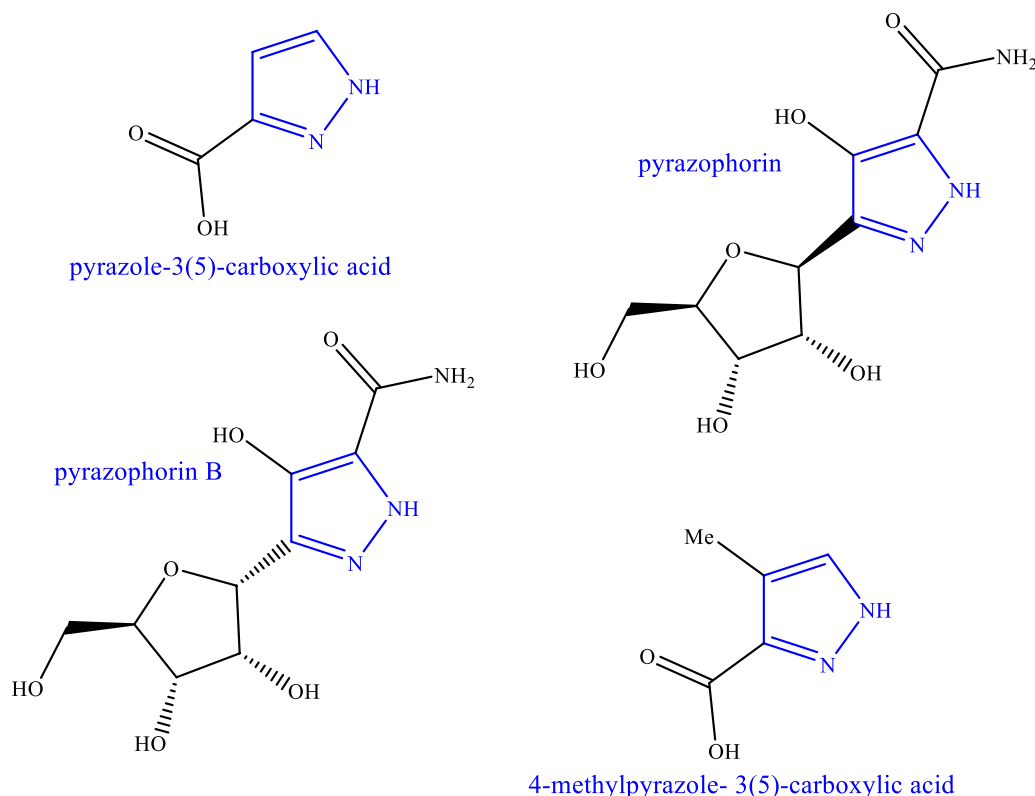
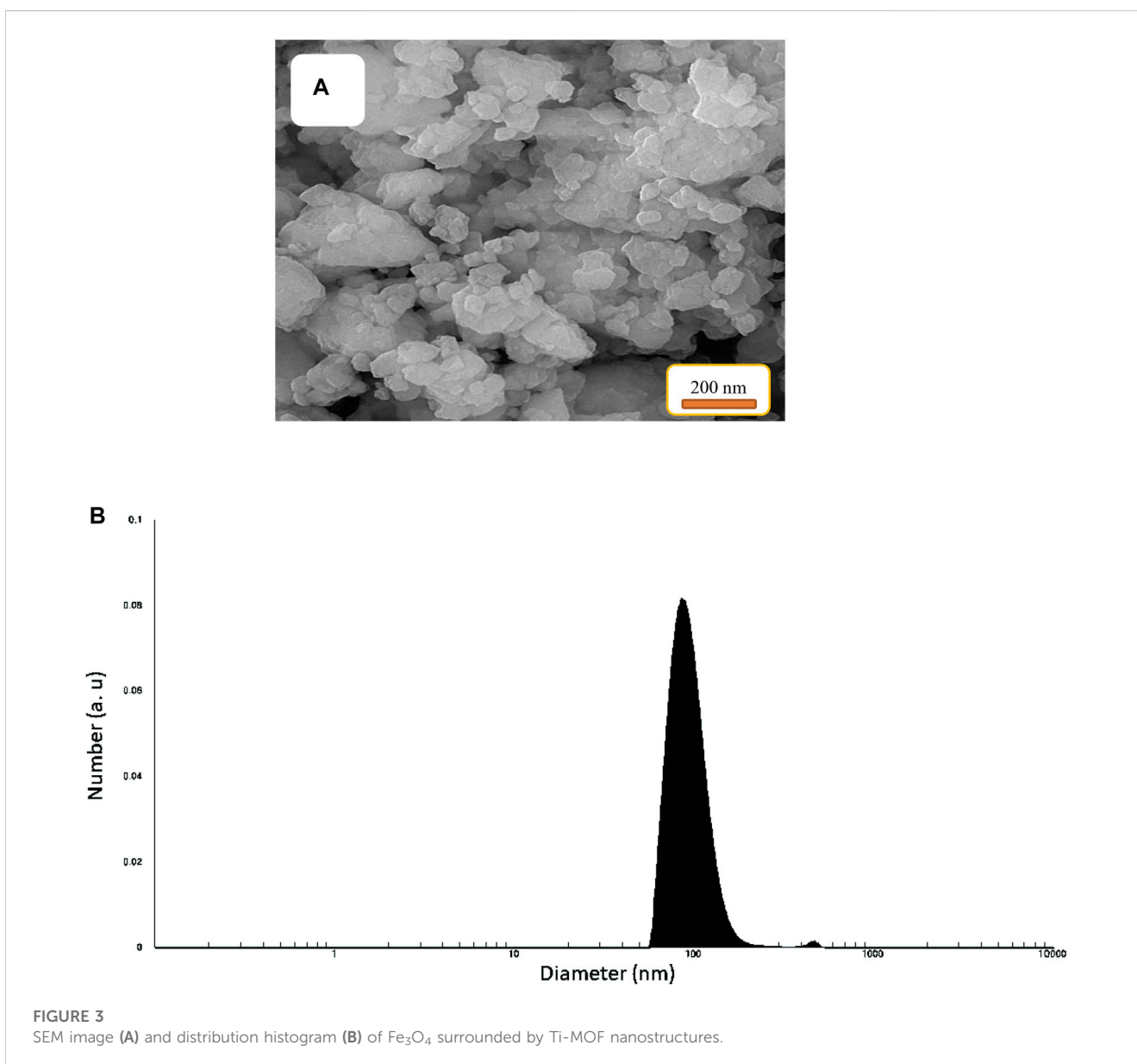
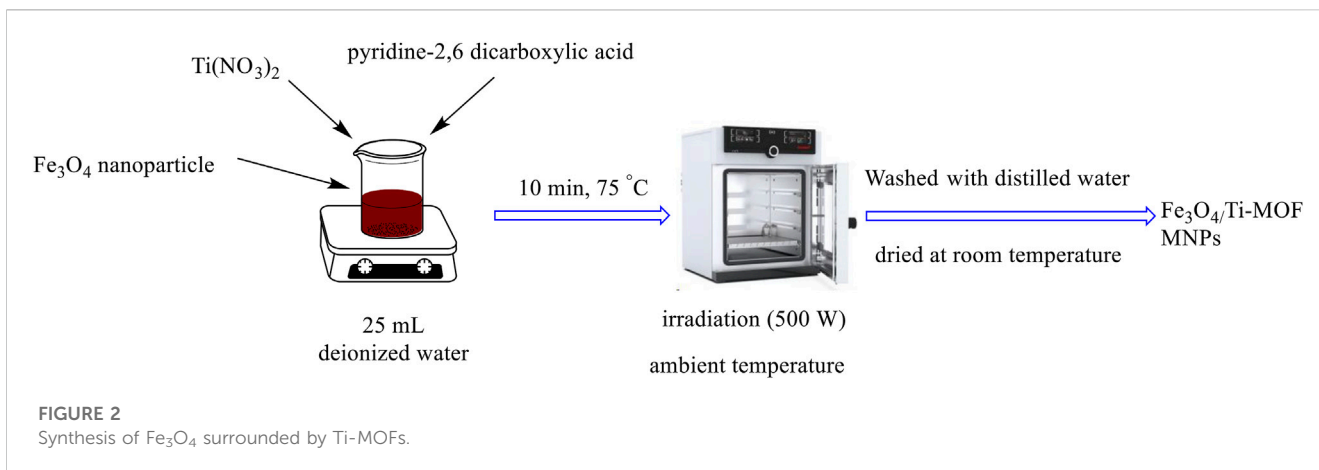


FIGURE 1
Pyrazole derivatives isolated from natural products.



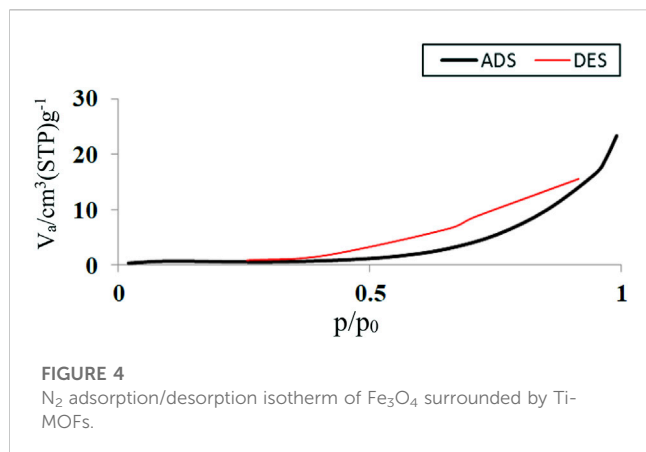


FIGURE 4
N₂ adsorption/desorption isotherm of Fe₃O₄ surrounded by Ti-MOFs.

point of view of medicinal chemistry, pyrazole heterocycles have a high potential for diversity-based organic synthesis (DOS) (Koehler, Shamji, and Schreiber, 2003).

To introduce this amount of diversity to the structure of chemical compounds, multicomponent reactions are the best possible tools (Sunderhaus and Martin, 2009; Syamala, 2009; Biggs-Houck, Younai, and Shaw, 2010).

Considering the importance of synthesizing heterocyclic compounds and reporting new methods, in this study, Fe₃O₄ surrounded by Ti-MOF nanostructures with the microwave method was synthesized. Fe₃O₄ surrounded by Ti-MOF nanostructures was

used as a recyclable and efficient magnetic nanocatalyst in the synthesis of pyrazole-4-carbonitrile derivatives.

In the continuation of investigations on the properties of Fe₃O₄ surrounded by Ti-MOF nanostructures, its antibacterial and antifungal activities were investigated, and significant results were observed.

2 Experiments

2.1 Materials and instruments

Solvents and chemical reagent from Merck were purchased. Fe₃O₄ nanostructures were purchased from Sigma-Aldrich.

The crystalline structures of the samples were investigated by X-ray powder diffraction (XRD, Rigaku SmartLab 9 kW) with a Cu-K α radiation source ($\lambda = 0.15406$ nm). The morphology and particle size distribution of the nanostructures were analyzed by scanning electron microscopy (SEM, Hitachi Regulus 8,100) at 3.0 kV. The physical properties of the catalysts were investigated by nitrogen adsorption-desorption characterization (Micromeritics AXAP 2460) performed at -196°C . The specific surface area was calculated using the BET equation, and the pore structure parameters were calculated from the BJH method.

The types of functional groups of the samples were tested by Fourier transform infrared spectra (FT-IR, Nicolet iS50) with a wave number range of $400\text{--}4,000\text{ cm}^{-1}$.

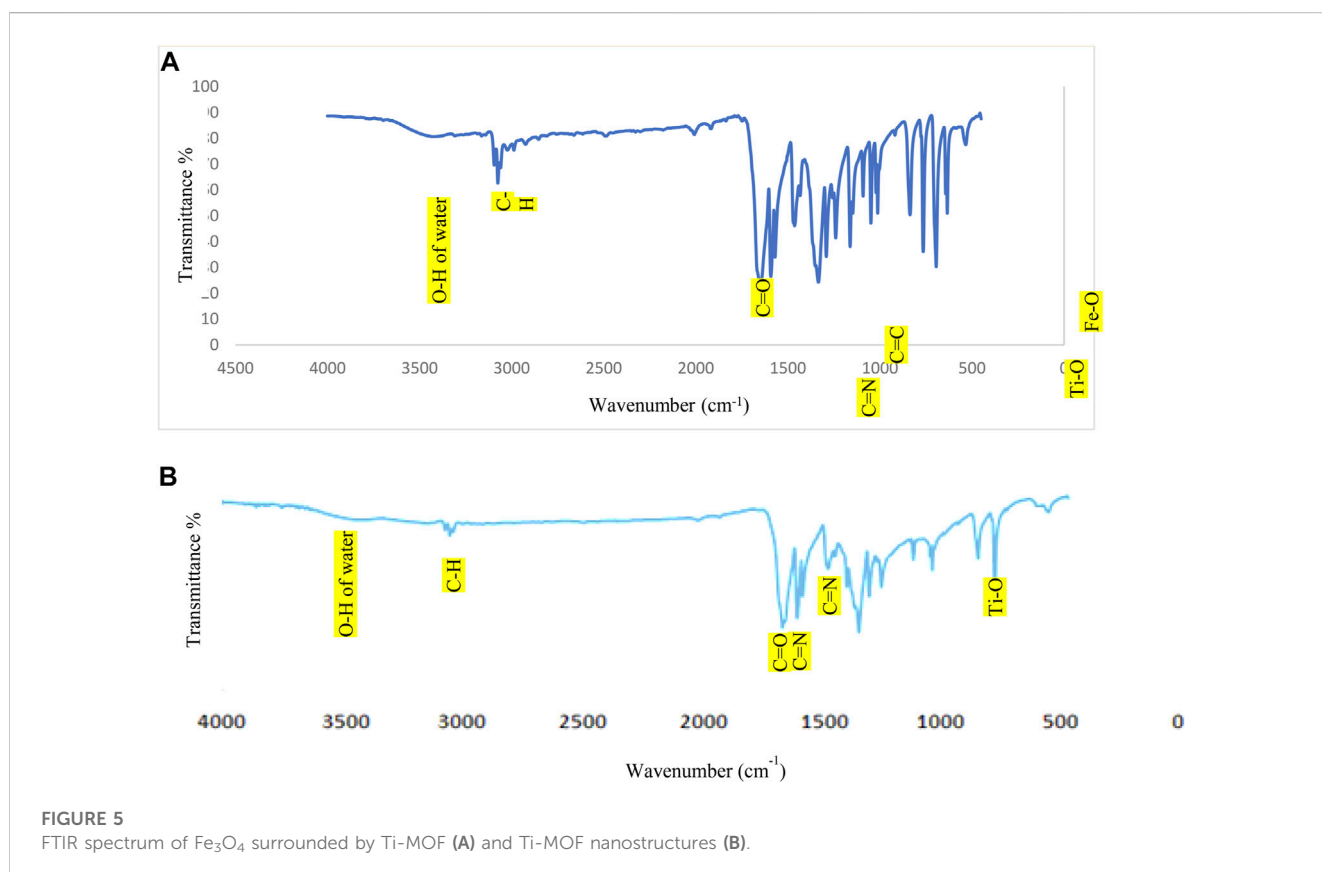
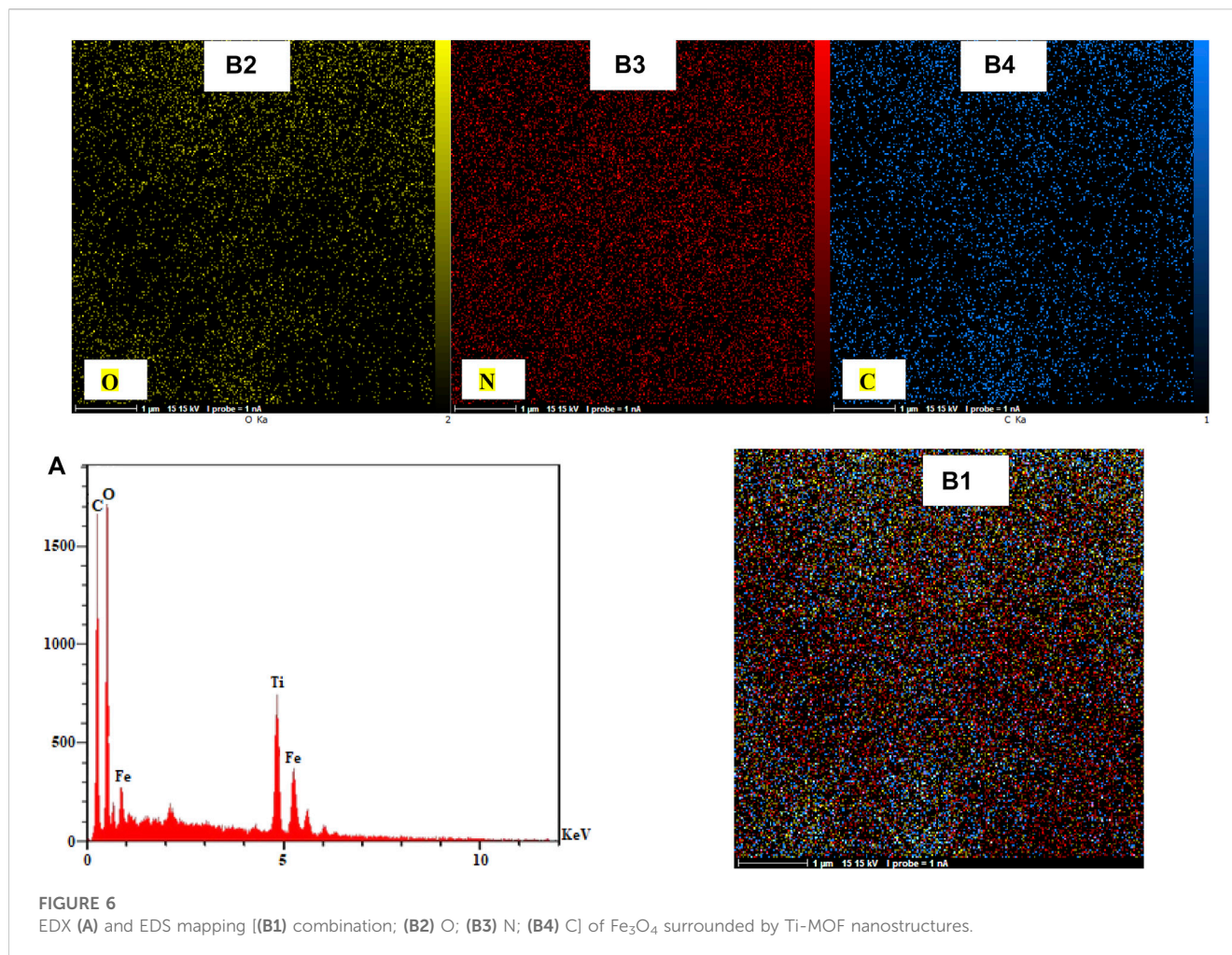


FIGURE 5
FTIR spectrum of Fe₃O₄ surrounded by Ti-MOF (A) and Ti-MOF nanostructures (B).



2.2 Synthesis of Fe₃O₄ surrounded by Ti-MOF nanostructures

A solution of 1 mmol Fe₃O₄ nanoparticle, 2 mmol Ti(NO₃)₄, and 2 mmol dipicolinic acid in 25 mL double-distilled water for 10 min at 75°C was stirred. Then, the mixture was put into the microwave reactor under irradiation (power of 500 W) at 25°C for 15 min. The products were cooled to room temperature. Finally, they were isolated and washed three times with deionized water/EtOH and dried at 25°C.

2.3 Synthesis of pyrazole-4-carbonitrile derivatives

For synthesizing pyrazole-4-carbonitrile derivatives, in 2 mL EtOH:H₂O (1:1), 1 mmol aromatic aldehydes, 1 mmol malononitrile, 1 mmol (2,4-dinitrophenyl)hydrazine, and 1 mg Fe₃O₄ surrounded by Ti-MOF nanostructures were added and stirred at 25°C. Reaction monitoring was performed by thin layer chromatography. After completion of the reaction, Fe₃O₄ surrounded by Ti-MOF nanostructures was separated by a magnet, and products were recrystallized in EtOH:H₂O.

2.3.1 5-Amino-1-(2,4-dinitrophenyl)-3-(4-fluorophenyl)-1H-pyrazole-4-carbonitrile (D2)

IR (KBr): 3,379, 3,319, 3,126, 3,042, 2,264, 1,621 cm⁻¹; ¹HNMR (DMSO-d₆, 400 MHz): δ= 7.52 (1H, d, J = 8.7 Hz), 7.61 (1H, d, J = 9.3 Hz), 7.79 (2H, d, J = 8.84 Hz), 7.86 (1H, d, J = 8.8 Hz), 7.90 (2H, d, J = 8.4 Hz), 8.61 (1H, s), and 8.76 (1H, s) ppm; ¹³CNMR (DMSO-d₆, 100 MHz): δ= 81.9, 114.9, 121.6, 122.7, 124.1, 128.5, 129.1, 129.4, 131.8, 133.7, 139.6, 148.2, 151.4, and 160.3 ppm; elemental analysis: C₁₆H₉FN₆O₄ calculated: C, 52.18; H, 2.46; N, 22.82; O, 17.38. Found: C, 52.25; H, 2.41; N, 22.79; O, 17.41.

2.3.2 5-Amino-3-(4-bromophenyl)-1-(2,4-dinitrophenyl)-1H-pyrazole-4-carbonitrile (D4)

IR (KBr): 3,386, 3,314, 3,135, 3,024, 2,247, and 1,626 cm⁻¹; ¹HNMR (DMSO-d₆, 400 MHz): δ= 7.49 (1H, d, J = 8.8 Hz), 7.63 (1H, d, J = 9.2 Hz), 7.75 (2H, d, J = 8.8 Hz), 7.85 (1H, d, J = 8.7 Hz), 7.95 (2H, d, J = 8.5 Hz), 8.64 (1H, s), and 8.71 (1H, s) ppm; ¹³CNMR (DMSO-d₆, 100 MHz): δ= 82.6, 115.3, 121.4, 122.3, 123.9, 128.9, 129.6, 129.9, 131.5, 134.1, 139.1, 148.6, 151.7, and 161.4 ppm; elemental analysis: C₁₆H₉BrN₆O₄ calculated: C, 44.78; H, 2.11; N, 19.58; O, 14.91. Found: C, 44.81; H, 2.09; N, 19.57; O, 14.93.

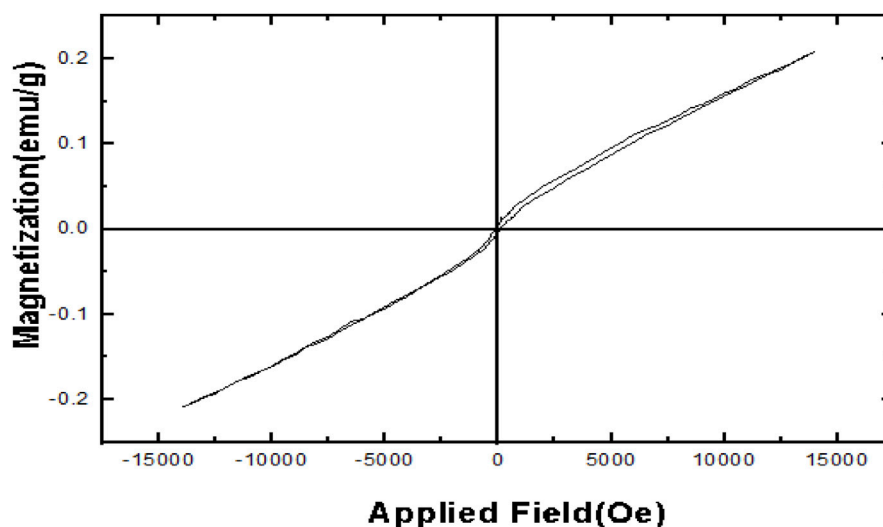


FIGURE 7
VSM curve of Fe_3O_4 surrounded by Ti-MOFs.

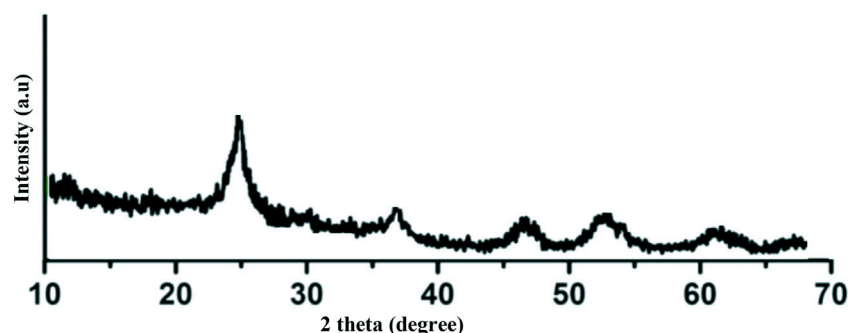


FIGURE 8
XRD patterns of Ti-MOF nanostructures.

2.3.3 5-Amino-1-(2,4-dinitrophenyl)-3-(4-nitrophenyl)-1H-pyrazole-4-carbonitrile (D6)

IR (KBr): 3,371, 3,331, 3,116, 3,047, 2,264, and 1,625 cm^{-1} ; ^1H NMR (DMSO- d_6 , 400 MHz): δ = 7.54 (1H, d, J = 8.6 Hz), 7.65 (1H, d, J = 9.1 Hz), 7.71 (2H, d, J = 8.7 Hz), 7.80 (1H, d, J = 8.4 Hz), 7.91 (2H, d, J = 8.4 Hz), 8.58 (1H, s), and 8.76 (1H, s) ppm; ^{13}C NMR (DMSO- d_6 , 100 MHz): δ = 83.61, 115.7, 121.8, 122.6, 124.3, 128.5, 129.1, 129.5, 131.2, 135.6, 140.1, 148.7, 153.6, and 162.1 ppm; elemental analysis: $\text{C}_{16}\text{H}_9\text{N}_7\text{O}_6$ calculated: C, 48.62; H, 2.30; N, 24.80; O, 24.28. Found: C, 48.59; H, 2.33; N, 24.84, O, 24.31.

2.4 Biological activity of Fe_3O_4 surrounded by Ti-MOF nanostructures

Biological activity of Fe_3O_4 surrounded by Ti-MOF nanostructures and antibacterial and antifungal activities based

on minimum inhibitory concentration (MIC), minimum bactericidal concentration (MBC), and minimum fungicidal concentration (MFC) values against Gram-negative bacterial strains and Gram-positive bacteria strains according to the CLSI guidelines M07-A9, M26-A, and M27-A2 were evaluated (Abdieva et al, 2022; Afrough et al, 2021; Zeraati et al, 2022; Hosseinzadegan et al, 2020a). In antimicrobial investigations, all tests were repeated three times, and the average results were reported.

3 Results and discussion

3.1 Synthesis identifies and confirms the structure of novel Fe_3O_4 surrounded by Ti-MOFs

In this study, Fe_3O_4 surrounded by Ti-MOF nanostructures was synthesized according to Figure 2.

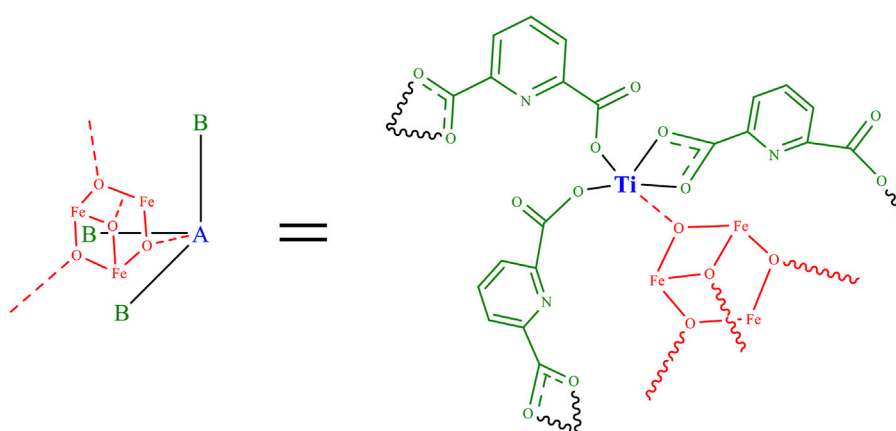
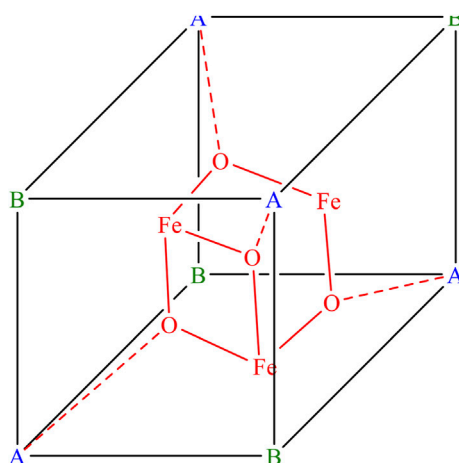
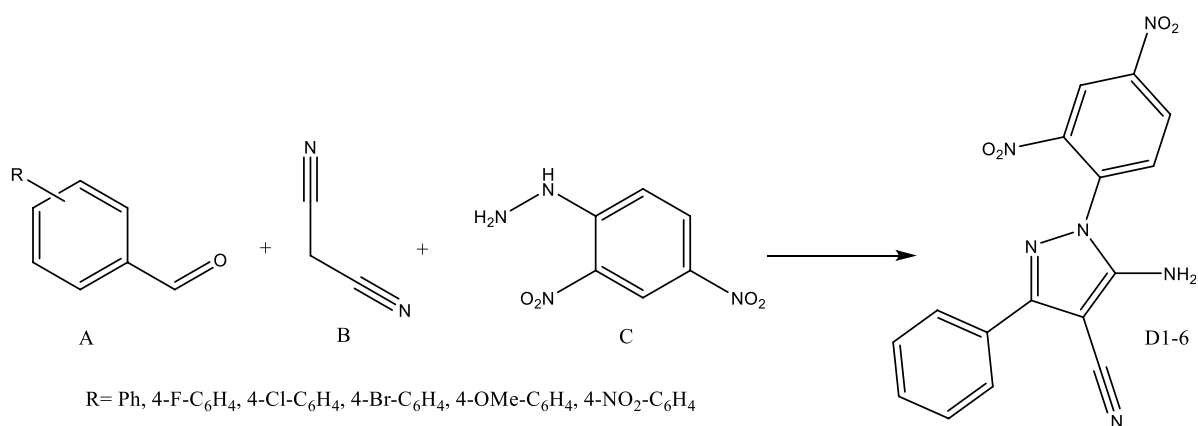


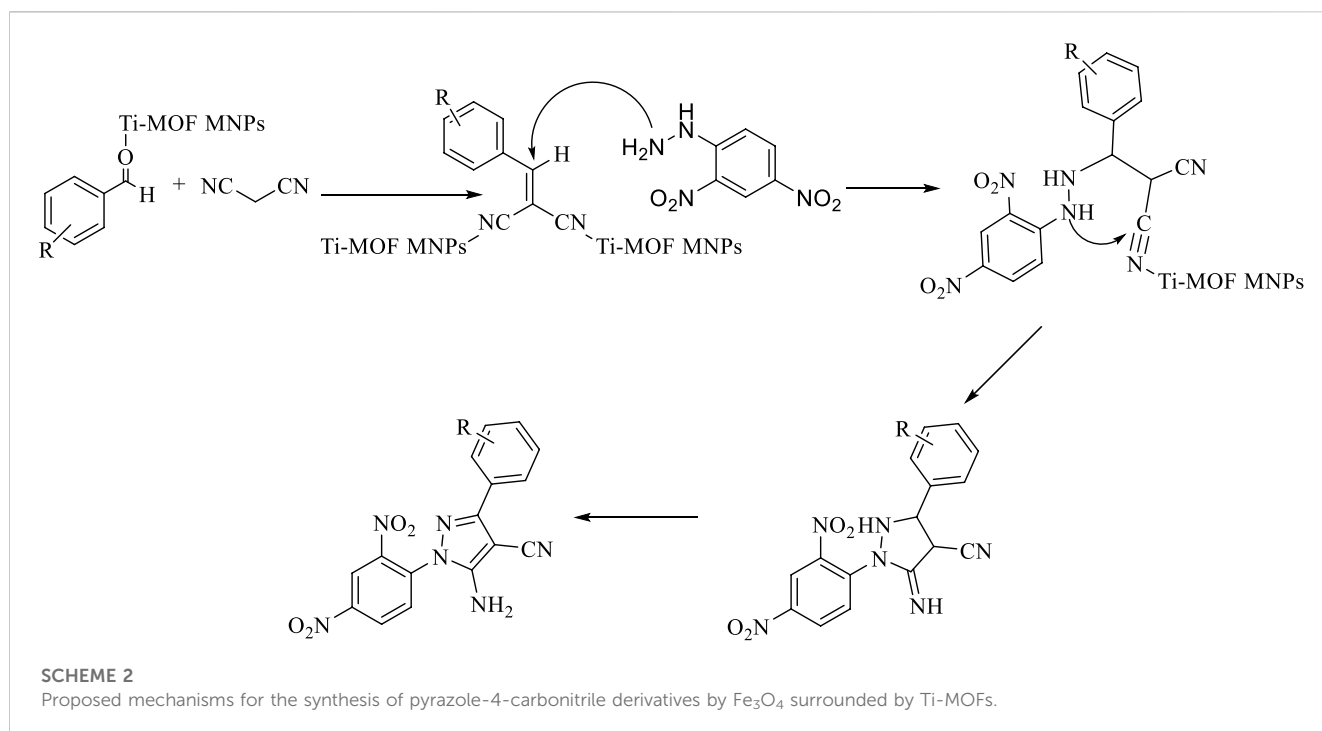
FIGURE 9
Proposed structure of Fe_3O_4 surrounded by Ti-MOF nanostructures.



SCHEME 1
 Fe_3O_4 surrounded by Ti-MOF nanostructures as magnetic nanocatalysts in the synthesis of pyrazole-4-carbonitrile derivatives.

To identify and confirm the structure of Fe_3O_4 surrounded by Ti-MOF nanostructures, related characterization techniques such as SEM, BET, EDX/EDX mapping, FT-IR, and VSM were used.

The morphology and particle size distribution of Fe_3O_4 surrounded by Ti-MOF nanostructures by SEM image (Figure 3) were investigated. According to this image, the morphology of Fe_3O_4 surrounded by Ti-MOF nanostructures was a uniform crystalline

**TABLE 1 Optimization of conditions in synthesizing D1.**

Entry	Amount catalyst (mg)	Solvent	Temperature ($^{\circ}\text{C}$)	Time (min)	Yield (%)
1	1	EtOH	r. t	60	64
2	2	EtOH	r. t	60	77
3	3	EtOH	r. t	45	85
4	4	EtOH	r. t	45	85
5	5	EtOH	r. t	45	81
6	3	$\text{H}_2\text{O}:\text{EtOH}$ (1:1)	r. t	30	93
7	3	MeOH	r. t	60	32
8	3	$\text{H}_2\text{O}:\text{EtOH}$ (1:1)	40	30	91
9	3	$\text{H}_2\text{O}:\text{EtOH}$ (1:1)	50	30	85

The bold values in the table indicate the optimal values obtained.

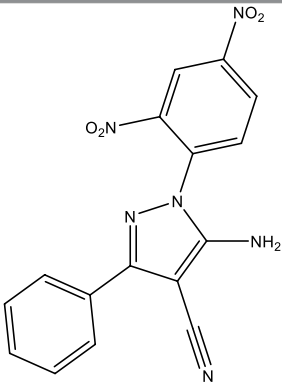
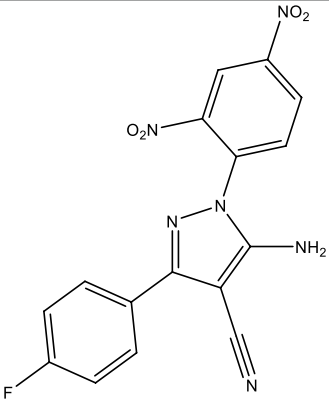
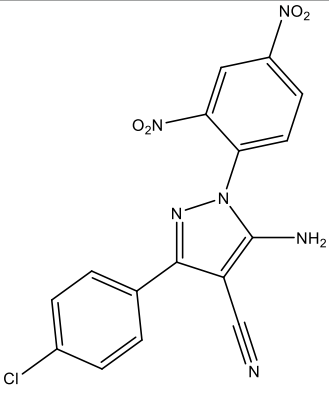
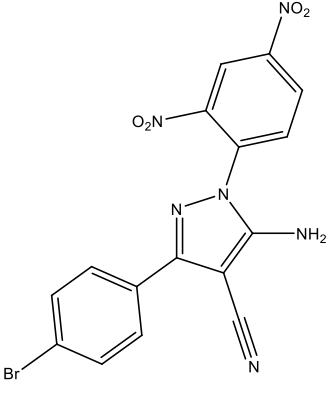
system with needle-shaped distribution. The homogeneous morphology with narrow particle size distribution of Fe_3O_4 surrounded by Ti-MOF nanostructures can be attributed to the efficient microwave-assisted synthesis under optimal conditions (microwave power: 500 W, temperature: 25°C , and time duration: 15 min). Compared to the previous sample (Moghaddam-manesh et al, 2022), the morphology of samples was homogeneous which can be related to the type of the synthesis method and also mild conditions of the microwave-assisted process. Particle size distribution of Fe_3O_4 surrounded by Ti-MOF nanostructures shows that the particles are in the nanorange, and the average particle size was 97 nm.

N_2 adsorption/desorption isotherms of synthesized Fe_3O_4 surrounded by Ti-MOF nanostructures are given in Figure 4.

BET results showed that Fe_3O_4 surrounded by Ti-MOF nanostructures has a specific surface area of approximately $37.500\text{ m}^2/\text{g}$. This amount-specific surface confirmed that Fe_3O_4 surrounded by Ti-MOF nanostructures has a desirable surface for catalytic reactions and biological agents. It means compared to the classical route (Zeraati et al, 2021), the microwave-assisted method has been influential on the synthesis of Fe_3O_4 surrounded by Ti-MOF nanostructures with potential specific surface area.

The FTIR spectrum of Fe_3O_4 surrounded by Ti-MOF nanostructures is given in Figure 5. In the FTIR spectrum of Fe_3O_4 surrounded by Ti-MOF nanostructures, the peak near $3,421\text{ cm}^{-1}$ was due to the hydration of water. The absorption near $3,000\text{ cm}^{-1}$ was due to C-H groups. The peak related to

TABLE 2 Synthesis of pyrazole-4-carbonitrile derivatives by Fe₃O₄ surrounded by Ti-MOFs.

Product	Structure	Time (min)	Yield (%)	Mp (°C)	
				Found	Reported
D1		30	93	224–226	225–227 (Aryan et al, 2017)
D2		20	91	248–251	New
D3		20	93	259–263	260–265 (Aryan et al, 2017)
D4		25	89	269–272	New

(Continued on following page)

TABLE 2 (Continued) Synthesis of pyrazole-4-carbonitrile derivatives by Fe₃O₄ surrounded by Ti-MOFs.

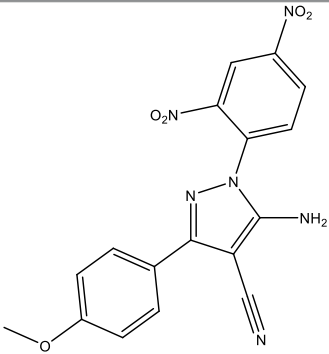
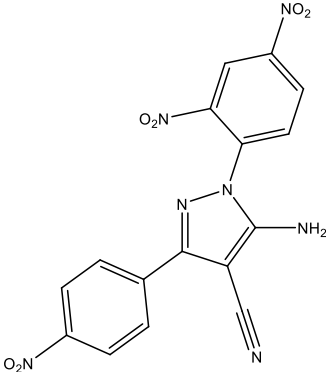
Product	Structure	Time (min)	Yield (%)	Mp (°C)	
				Found	Reported
D5		25	93	154–156	154–155 (M'Hamed and Alduaij, 2016)
D6		15	94	231–232	New

TABLE 3 Synthesis of pyrazole-4-carbonitrile derivatives under different conditions.

Entry	Condition	Time (min)	Temperature (°C)	Yield (%)
1	Glucose:urea, deep eutectic solvent	50	r. t	89 (Aryan et al, 2017)
2	Through ball milling	40	r. t	93
3	This work	30	r. t	93

carbonyl groups and C=N was near 1,600 cm⁻¹ and 1,550 cm⁻¹, respectively. (Bakhshi et al, 2022). The absorption due to C=C groups was shown near 1,400 cm⁻¹. The absorption values related to Ti–O and Fe–O were given near 670 cm⁻¹ (Al-Amin et al, 2016) and 530 cm⁻¹ (Hosseinzadegan, Hazeri, and Maghsoodlou, 2020b), respectively.

Based on the FTIR spectrum, the peaks and absorption of a group present in the structure of Fe₃O₄ surrounded by Ti-MOF nanostructures were observed.

The EDX and EDS mapping proved the presence of elements and compounds used in synthesizing Fe₃O₄ surrounded by Ti-MOF nanostructures. The elements of Fe, C, O, and N in EDX and EDS mapping were observed. These elements were in the structure of reactants. EDX and EDS mapping of Fe₃O₄ surrounded by Ti-MOF nanostructures are given in Figure 6. According to these analyses,

the related elements were distributed as homogeneous which confirmed the successful dispersion of Fe₃O₄ elements surrounded by Ti-MOF nanostructures.

The magnetic saturation of Fe₃O₄ surrounded by Ti-MOF nanostructures is given in the curve of Figure 7. The magnetic saturation value for Fe₃O₄ surrounded by Ti-MOF nanostructures was 0.022 emu/g. Magnetic saturation for Fe₃O₄ MNPs was 0.055 emu/g (Hosseinzadegan et al, 2020a). Reduction of magnetic saturation in Fe₃O₄ surrounded by Ti-MOF nanostructures proves the presence of Ti-MOF particles around Fe₃O₄.

The magnetism of Fe₃O₄ surrounded by Ti-MOF nanostructures makes them easy to separate after performing the desired reactions by magnets, which was another feature of synthesized Fe₃O₄ surrounded by Ti-MOF nanostructures.

TABLE 4 Antibacterial and antifungal activities of Fe₃O₄ surrounded by Ti-MOF and comparison with commercial drugs.

MNPs/commercial drug	Gram-negative bacteria strain				Gram-positive bacteria strain				Fungi strain			
	<i>Shigella dysenteriae</i>		<i>Klebsiella pneumoniae</i>		<i>Bacillus cereus</i>		<i>Staphylococcus epidermidis</i>		<i>Fusarium oxysporum</i>		<i>Candida albicans</i>	
	MIC	MBC	MIC	MBC	MIC	MBC	MIC	MBC	MIC	MBC	MIC	MBC
MNPs	128	256	32	128	32	64	16	32	128	256	64	128
Cefazolin	—	—	1	2	—	—	1	2	N.C	N.C	N.C	N.C
Gentamicin	32	64	4	8	1	4	2	4	N.C	N.C	N.C	N.C
Tolnaftate	N.C	N.C	N.C	N.C	N.C	N.C	N.C	N.C	64	128	32	64
Terbinafine	N.C	N.C	N.C	N.C	N.C	N.C	N.C	N.C	-	-	-	-

N. C, not checked.

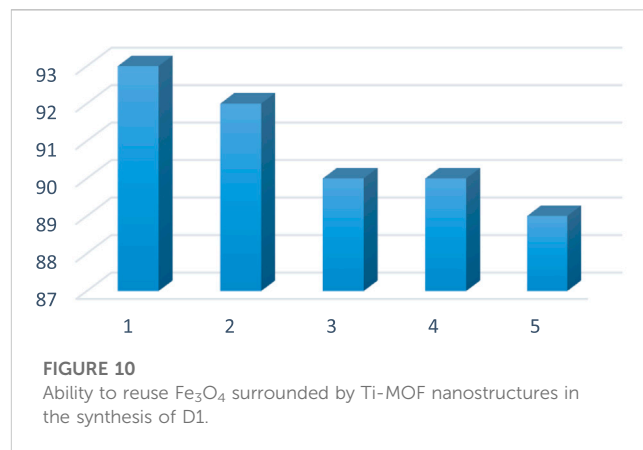


FIGURE 10 Ability to reuse Fe₃O₄ surrounded by Ti-MOF nanostructures in the synthesis of D1.

Figure 8 shows the XRD patterns of Fe₃O₄ surrounded by Ti-MOF nanostructures. According to this image, the patterns related to the formation of Fe₃O₄ surrounded by Ti-MOF nanostructures were successfully conformed. Furthermore, according to the Debye–Scherer equation, the mean crystalline size is approximately 91 nm. The width of peaks confirmed the narrow crystalline size distribution of final products. The crystalline behavior of Fe₃O₄ surrounded by Ti-MOF nanostructures was in agreement with the previous literature (Li et al, 2019).

Based on the spectral data and analyzed, Figure 9 is proposed for Fe₃O₄ surrounded by Ti-MOF nanostructures.

3.2 Synthesis of pyrazole-4-carbonitrile derivatives by Fe₃O₄ surrounded by Ti-MOF nanostructures

Fe₃O₄ surrounded by Ti-MOF nanostructures was used as magnetic catalysts to synthesize pyrazole-4-carbonitrile derivatives based on Scheme 1.

The first step in the synthesis of derivatives was optimization of the reaction conditions. According to Table 1, for 5-amino-1-(2,4-dinitrophenyl)-3-phenyl-1H-pyrazole-4-carbonitrile (D1), milligrams of catalyst, solvent and temperature were optimized.

In 3 mg of catalyst, 1 to 1 H₂O:EtOH as a solvent, ambient temperature, and high efficiency were observed, and other derivatives listed in Table 2 were synthesized using optimal conditions.

Derivatives D2, D4, and D6 were new compounds synthesized in this study. In Scheme 2, the proposed mechanism for the synthesis of derivatives is presented.

One of the factors that made Fe₃O₄ surrounded by Ti-MOF nanostructures important in synthesizing pyrazole-4-carbonitrile derivatives was their recyclability. After synthesizing the products, the catalyst with H₂O and EtOH was washed and dried at ambient temperature under vacuum. After drying, it was used again in the synthesis of derivatives. Investigations proved that magnetic nanoparticles could be used up to five times without significantly reducing efficiency in the synthesis of D1 (Figure 10).

Since (2,4-dinitrophenyl)hydrazine has low reactivity, so far, two methods have been reported for the synthesis of pyrazole-4-carbonitrile derivatives using 2 (2,4-dinitrophenyl)hydrazine as a reagent, and the results are given in Table 3.

Based on the results of Table 3, the catalysts used in this study, in addition to convenient synthesis conditions of derivatives and synthesis of novel derivatives, took less time and had higher efficiency.

Although the magnetic MOF structures similar to the synthesized compound in this study have been reported so far, the difference between this study and the previous report is the use of different metals. In this study, titanium was used, but in the reported study, molybdenum was used. In addition, in the previous report, the synthesized Fe₃O₄/Mo-MOF compound was used as a catalyst in the synthesis of pyrano [2,3-d]pyrimidine derivatives, but Fe₃O₄ surrounded by Ti-MOF nanostructures synthesized in this study was used for the synthesis of pyrazole derivatives (Abdtawfeeq et al, 2022).

3.3 Biological activity results of Fe₃O₄ surrounded by Ti-MOF nanostructures

Antibacterial and antifungal activities of Fe₃O₄ surrounded by Ti-MOF nanostructures as biological activity were studied. MIC, MFC, and MBC values on Gram-negative bacterial species including *Shigella dysenteriae* and *Klebsiella pneumoniae*; Gram-positive bacteria species including *Bacillus cereus* and *Staphylococcus epidermidis*; and fungi strains including *Fusarium oxysporum* and *Candida albicans* for Fe₃O₄ surrounded by Ti-MOF nanostructures were studied (Table 4).

Based on previous studies, compounds containing titanium have significant antimicrobial and antibacterial properties (He et al, 2017; Azizi-Lalabadi et al, 2019). In this study, it was found that Fe₃O₄ surrounded by Ti-MOF nanostructures affects all studied bacterial strains, Gram-positive bacterial strains, and fungal strains that its high effectiveness can be attributed to the presence of titanium in its structure. As mentioned in Sections 1–2, the high specific surface area of Fe₃O₄ surrounded by Ti-MOF nanostructures was also influential in its antibacterial and antifungal activity. A comparison of the antibacterial and antifungal properties of Fe₃O₄ surrounded by Ti-MOF nanostructures with cefazolin, gentamicin, tolnaftate, and terbinafine showed that synthesized Fe₃O₄ surrounded by Ti-MOF nanostructures has a higher effect on *Shigella dysenteriae*, *Bacillus cereus* (bacterial strains), *Fusarium oxysporum*, and *Candida albicans* (fungal strain) than cefazolin (antibacterial) and terbinafine (antifungal), which were known as a commercial antibacterial and antifungal drugs (Potbhare et al, 2019; Chouke, Dadure, et al, 2022a; Chouke, Shrirame, et al, 2022b).

4 Conclusion

In short, novel Fe₃O₄ surrounded by Ti-MOF nanostructures using the microwave method was synthesized, and their structure was identified and confirmed by SEM, BET, FT-IR, EDX/EDX mapping, and VSM. Analysis of SEM and BET showed that the microwave method has the uniformity of morphology and specific surface area of Fe₃O₄ surrounded by Ti-MOF nanostructures, which can increase its catalytic and biological properties and continue to be discussed. Fe₃O₄ surrounded by Ti-MOF nanostructures was used as a recyclable and efficient catalyst in synthesizing pyrazole-4-carbonitrile derivatives and proved that derivatives were synthesized under better conditions than the previously presented methods. Derivatives were synthesized in 15–30 min with the efficiency of 89%–94%. Three new pyrazole

derivatives were synthesized and identified by spectral data. Another advantage of using Fe₃O₄ surrounded by Ti-MOF nanostructures as a catalyst was its easy separation after completion of the reaction by a magnet. In the continuation of our research on Fe₃O₄ surrounded by Ti-MOF nanostructures, its antibacterial and antifungal activities were evaluated, and significant results were observed. The minimum inhibitory concentration for the derivatives on the studied bacterial and fungal species was observed between 16 and 128 µg/mL. In some of the studied strains, higher effectiveness than known commercial drugs was also observed, which can be attributed to the presence of titanium and high specific surface area of it.

Data availability statement

The original contributions presented in the study are included in the article/Supplementary Material; further inquiries can be directed to the corresponding author.

Author contributions

Conceptualization, BQ and ZA; methodology, SF; form analysis, HC; investigation, ZA; resources, UA; data curation, ZA; writing—original draft preparation, SH; writing—review and editing, ZA, MS and MYA; supervision, IW; project administration, RS; funding acquisition, BQ. All authors contributed to the article and approved the submitted version.

Acknowledgments

The authors express their gratitude to the Deanship of Scientific Research at King Khalid University for funding this work through the Large Research Group Project under grant number RGP.02/214/43.

Conflict of interest

The authors declare that the research was conducted in the absence of any commercial or financial relationships that could be construed as a potential conflict of interest.

Publisher's note

All claims expressed in this article are solely those of the authors and do not necessarily represent those of their affiliated organizations, or those of the publisher, the editors, and the reviewers. Any product that may be evaluated in this article, or claim that may be made by its manufacturer, is not guaranteed or endorsed by the publisher.

Supplementary material

The Supplementary Material for this article can be found online at: <https://www.frontiersin.org/articles/10.3389/fmats.2023.1156702/full#supplementary-material>

References

- Abd El Salam, H., and Sharara, T. (2019). A novel microwave synthesis of manganese based MOF for adsorptive of Cd (II), Pb (II) and Hg (II) ions from aqua medium. *Egypt. J. Chem.* 62 (5), 0–851. doi:10.21608/ejchem.2019.6524.1550
- Abdel-Aziz, M., Abuo-Rahma, G. E.-D. A., and Hassan, A. A. (2009). Synthesis of novel pyrazole derivatives and evaluation of their antidepressant and anticonvulsant activities. *Eur. J. Med. Chem.* 44 (9), 3480–3487. doi:10.1016/j.ejmech.2009.01.032
- Abdi, J., Abdollah Jamal SisiHadipoor, M., and Khataee, A. (2022). State of the art on the ultrasonic-assisted removal of environmental pollutants using metal-organic frameworks. *J. Hazard. Mater.* 424, 127558. doi:10.1016/j.jhazmat.2021.127558
- Abdieva, G. A., Patra, I., Al-Qargholi, B., Shahryari, T., Narendra Pal Singh Chauhanand Moghaddam-Manesh, M. (2022). An efficient ultrasound-assisted synthesis of Cu/Zn hybrid MOF nanostructures with high microbial strain performance. *Front. Bioeng. Biotechnol.* 10, 861580. doi:10.3389/fbioe.2022.861580
- Abdtawfeeq, T. H., Farhan, Z. A., Al-Majidi, K., Mohammed Abed JawadZabibah, R. S., Riadi, Y., et al. (2022). Ultrasound-assisted and one-pot synthesis of new Fe₃O₄/Mo-MOF magnetic nano polymer as a strong antimicrobial agent and efficient nanocatalyst in the multicomponent synthesis of novel Pyran [2, 3-d] pyrimidines derivatives. *J. Inorg. Organomet. Polym. Mater.* 33, 472–483. doi:10.1007/s10904-022-02514-7
- Afrough, T., Bakavoli, M., Eshghi, H., Hamid, B., and Moghaddam-Manesh, M. (2021). Synthesis, characterization and *in vitro* antibacterial evaluation of novel 4-(1-(Pyrimidin-4-yl) ethyl)-12 H-pyrimido [4', 5': 5, 6] [1, 4] thiazino [2, 3-b] quinoxaline derivatives. *Polycycl. Aromat. Compd.* 41 (4), 735–745. doi:10.1080/10406638.2019.1614640
- Aghaee, M., Mohammadi, K., Hayati, P., Sharafi-Badr, P., Yazdian, F., Gutierrez Alonso, A., et al. (2022). A novel 3D Ag (I) metal-organic coordination polymer (Ag-MOCP): Crystallography, Hirshfeld surface analysis, antibacterial effect and molecular docking studies. *J. Solid State Chem.* 310, 123013. doi:10.1016/j.jssc.2022.123013
- Akbari, Z., Montazerzohori, M., Naghiha, R., Hayati, P., Micale, N., Cristani, M., et al. (2022). Some new antimicrobial/antioxidant nanostructure zinc complexes: Synthesis, crystal structure, Hirshfeld surface analyses and thermal behavior. *Results Chem.* 4, 100636. doi:10.1016/j.rechem.2022.100636
- Al-AminMohammadDey, S. C., Taslim Ur RashidMd Ashaduzzamanand Sayed Md Shamsuddin (2016). Solar assisted photocatalytic degradation of reactive azo dyes in presence of anatase titanium dioxide. *Int. J. Latest Res. Eng. Technol.* 2 (3), 14–21.
- Aryan, R., Hamid, B., Nojavan, M., and Rezaei, M. (2017). Novel biocompatible glucose-based deep eutectic solvent as recyclable medium and promoter for expedient multicomponent green synthesis of diverse three and four substituted pyrazole-4-carbonitrile derivatives. *Res. Chem. Intermed.* 43 (8), 4731–4744. doi:10.1007/s11164-017-2908-5
- Asghar, A., Iqbal, N., and Noor, T. (2020). Ultrasonication treatment enhances MOF surface area and gas uptake capacity. *Polyhedron* 181, 114463. doi:10.1016/j.poly.2020.114463
- Azizi-Lalabadi, M., Ali, E., Divband, B., and Alizadeh-Sani, M. (2019). Antimicrobial activity of Titanium dioxide and Zinc oxide nanoparticles supported in 4A zeolite and evaluation the morphological characteristic. *Sci. Rep.* 9 (1), 17439–17510. doi:10.1038/s41598-019-54025-0
- Bakhshi, A., Saravani, H., Rezvani, A., Sargazi, G., and Shahbakhsh, M. (2022). A new method of Bi-MOF nanostructures production using UAIM procedure for efficient electrocatalytic oxidation of aminophenol: A controllable systematic study. *J. Appl. Electrochem.* 52, 709–728. doi:10.1007/s10800-021-01664-9
- Bendaha, H., Yu, L., Touzani, R., Souane, R., Giaever, G., Corey, N., et al. (2011). New azole antifungal agents with novel modes of action: Synthesis and biological studies of new tridentate ligands based on pyrazole and triazole. *Eur. J. Med. Chem.* 46 (9), 4117–4124. doi:10.1016/j.ejmech.2011.06.012
- Biggs-HouckJames, E., Younai, A., and Shaw, J. T. (2010). Recent advances in multicomponent reactions for diversity-oriented synthesis. *Curr. Opin. Chem. Biol.* 14 (3), 371–382. doi:10.1016/j.cbpa.2010.03.003
- Chouke, P. B., Dadure, K. M., Potbhare, A. K., Bhusari, G. S., Mondal, A., Chaudhary, K., et al. (2022a). Biosynthesized δ -Bi₂O₃ nanoparticles from *Crinum viviparum* flower extract for photocatalytic dye degradation and molecular docking. *ACS omega* 7 (24), 20983–20993. doi:10.1021/acsomega.2c01745
- Chouke, P. B., Shrirame, T., Potbhare, A. K., Mondal, A., Chaudhary, A. R., Mondal, S., et al. (2022b). Bioinspired metal/metal oxide nanoparticles: A road map to potential applications. *Mater. Today Adv.* 16, 100314. doi:10.1016/j.mtadv.2022.100314
- Sabbagh, E., Osama, I., Baraka, M. M., Ibrahim, S. M., Pannecouque, C., Andrei, G., et al. (2009). Synthesis and antiviral activity of new pyrazole and thiazole derivatives. *Eur. J. Med. Chem.* 44 (9), 3746–3753. doi:10.1016/j.ejmech.2009.03.038
- Eshghi, F., Mehrabadi, Z., Farsadrooh, M., Hayati, P., Javadian, H., Karimi, M., et al. (2023). Photocatalytic degradation of remdesivir nucleotide pro-drug using [Cu (1-methylimidazole) 4 (SCN) 2] nanocomplex synthesized by sonochemical process: Theoretical, hirshfeld surface analysis, degradation kinetic, and thermodynamic studies. *Environ. Res.* 222, 115321. doi:10.1016/j.envres.2023.115321
- Farsi, R., Mohammadi, M. K., and Seyyed Jafar Saghanezhad (2021). Sulfonamide-functionalized covalent organic framework (COF-SO 3 H): An efficient heterogeneous acid catalyst for the one-pot preparation of polyhydroquinoline and 1, 4-dihydropyridine derivatives. *Res. Chem. Intermed.* 47, 1161–1179. doi:10.1007/s11164-020-04322-5
- Gouda, M. A., Ma, B., Shoeib, A. I., and Khalil, A. M. (2010). Synthesis and antimicrobial of new anthraquinone derivatives incorporating pyrazole moiety. *Eur. J. Med. Chem.* 45 (5), 1843–1848. doi:10.1016/j.ejmech.2010.01.021
- GranetoMatthew, J., Kurumbail, R. G., Vazquez, M. L., Sheng Shieh, H., JenniferPawlit, L., et al. (2007). Synthesis, crystal structure, and activity of pyrazole-based inhibitors of p38 kinase. *J. Med. Chem.* 50 (23), 5712–5719. doi:10.1021/jm0611915
- He, X., Zhang, X., Wang, X., and Qin, L. (2017). Review of antibacterial activity of titanium-based implants' surfaces fabricated by micro-arc oxidation. *Coatings* 7 (3), 45. doi:10.3390/coatings7030045
- Hosseinazadegan, S., Hazeri, N., Malek Taher MaghsoodlouMoghaddam-Manesh, M., and Shirzaei, M. (2020b). Synthesis and evaluation of biological activity of novel chromeno [4, 3-b] quinolin-6-one derivatives by SO 3 H-tryptamine supported on Fe 3 O 4@ SiO 2@ CPS as recyclable and bioactive magnetic nanocatalyst. *J. Iran. Chem. Soc.* 17 (12), 3271–3284. doi:10.1007/s13738-020-01990-3
- Hosseinazadegan, S., Hazeri, N., and Malek Taher Maghsoodlou (2020a). Synthesis of novel thiazolo [3, 2-a] chromeno [4, 3-d] pyrimidine-6 (7H)-ones by bioactive Fe₃O₄@ gly@ thiophen@ Cu (NO₃)₂ as reusable magnetic nanocatalyst. *Appl. Organomet. Chem.* 34 (9), e5797. doi:10.1002/aoc.5797
- Karimi, M., Mehrabadi, Z., Farsadrooh, M., Bafkary, R., Derikvandi, H., Hayati, P., et al. (2021). "Metal-organic framework," in *Interface science and Technology* (Amsterdam, Netherlands: Elsevier), 279–387.
- Karimipour, Z., Reza Jalilzadeh YengejehHaghighatzadeh, A., Mohammadi, M. K., and Rouzbehani, M. M. (2021). UV-induced photodegradation of 2, 4, 6-trichlorophenol using Ag-Fe 2 O 3-CeO 2 photocatalysts. *J. Inorg. Organomet. Polym. Mater.* 31, 1143–1152. doi:10.1007/s10904-020-01859-1
- Koehler, A. N., Shamji, A. F., and Schreiber, S. L. (2003). Discovery of an inhibitor of a transcription factor using small molecule microarrays and diversity-oriented synthesis. *J. Am. Chem. Soc.* 125 (28), 8420–8421. doi:10.1021/ja0352698
- Kryštof, V., Cankář, P., Fryšová, I., Jan, S., George, K., Džubák, P., et al. (2006). 4-Arylazo-3, 5-diamino-1 H-pyrazole CDK inhibitors: SAR study, crystal structure in complex with CDK2, selectivity, and cellular effects. *J. Med. Chem.* 49 (22), 6500–6509. doi:10.1021/jm0605740
- Kumar, H., Saini, D., Jain, S., and Jain, N. (2013a). Pyrazole scaffold: A remarkable tool in the development of anticancer agents. *Eur. J. Med. Chem.* 70, 248–258. doi:10.1016/j.ejmech.2013.10.004
- Kumar, V., Kaur, K., Gupta, G. K., and Sharma, A. K. (2013b). Pyrazole containing natural products: Synthetic preview and biological significance. *Eur. J. Med. Chem.* 69, 735–753. doi:10.1016/j.ejmech.2013.08.053
- Li, C.-H., Huang, C.-L., Chuah, X.-F., Duraisamy Senthil RajaHsieh, C.-T., and Lu, S.-Y. (2019). Ti-MOF derived TixFe1-xOy shells boost Fe₂O₃ nanorod cores for enhanced photoelectrochemical water oxidation. *Chem. Eng. J.* 361, 660–670. doi:10.1016/j.cej.2018.12.097
- M'HamedMohamed, O., and OmarAlduaij, K. (2016). Green and effective one-pot synthesis of 5-Oxo-pyrazolidine and 5-Amino-2, 3-dihydro-1H-Pyrazole derivatives through Ball Milling under catalyst-free and solvent-free conditions. *Asian J. Chem.* 28 (3), 543–547. doi:10.14233/ajchem.2016.19397
- Mitchell, L. H., Drew, A. E., ScottRibich, A., Rioux, N., Swinger, K. K., Jacques, S. L., et al. (2015). Aryl pyrazoles as potent inhibitors of arginine methyltransferases: Identification of the first PRMT6 tool compound. *ACS Med. Chem. Lett.* 6 (6), 655–659. doi:10.1021/acsmchemlett.5b00071
- Moghaddam-manesh, M., Sargazi, G., Roohani, M., Nooshin Gholipour ZanjaniKhaleghi, M., and Hosseinazadegan, S. (2022). Synthesis of PVA/Fe₃O₄@ SiO₂@ CPS@ SiO₂@ Ni as novel magnetic fibrous composite polymer nanostructures and evaluation of anti-cancer and antimicrobial activity. *Polym. Bull.*, 1–12. doi:10.1007/s00289-022-04584-6
- Potbhare, A. K., Ratiram Gomaji ChaudharyChouke, P. B., Yerpude, S., Mondal, A., Sonkusare, V. N., et al. (2019). Phytosynthesis of nearly monodisperse CuO nanospheres using *Phyllanthus reticulatus/Conyza bonariensis* and its antioxidant/antibacterial assays. *Mater. Sci. Eng. C* 99, 783–793. doi:10.1016/j.msec.2019.02.010

Sharafi-Badr, P., Hayati, P., and Mahmoudi, G. (2022). "Biological MOFs (bio-MOFs) for energy applications," in *Metal-organic framework-based nanomaterials for energy conversion and storage* (Amsterdam, Netherlands: Elsevier), 81–103.

Sunderhaus, J. D., and Martin, S. F. (2009). Applications of multicomponent reactions to the synthesis of diverse heterocyclic scaffolds. *Chemistry–A Eur. J.* 15 (6), 1300–1308. doi:10.1002/chem.200802140

Syamala, M. (2009). Recent progress in three-component reactions. An update. *Org. Prep. Proced. Int.* 41 (1), 1–68. doi:10.1080/00304940802711218

Van Herk, T. J. B., Amch Van den Nieuwendijk Van Der Klein, P. A. M., Ijzerman, A. P., Stannek, C., Burmeister, A., et al. (2003). Pyrazole derivatives as partial agonists for the nicotinic acid receptor. *J. Med. Chem.* 46 (18), 3945–3951. doi:10.1021/jm030888c

Zeraati, M., Ali, M., Vafaei, S., Narendra Pal Singh Chauhan and Sargazi, G. (2021). Taguchi-assisted optimization technique and density functional theory for green synthesis of a novel Cu-MOF derived from caffeic acid and its anticancerous activities. *Front. Chem.*, 972. doi:10.3389/fchem.2021.722990

Zeraati, M., Moghaddam-Manesh, M., Khodamoradi, S., Hosseinzadegan, S., Golpayegani, A., Narendra Pal Singh Chauhan, et al. (2022). Ultrasonic assisted reverse micelle synthesis of a novel Zn-metal organic framework as an efficient candidate for antimicrobial activities. *J. Mol. Struct.* 1247, 131315. doi:10.1016/j.molstruc.2021.131315

Zhou, J.-J., Ji, W., Xu, L., Yang, Y., Wang, W., Ding, H., et al. (2022). Controllable transformation of CoNi-MOF-74 on Ni foam into hierarchical-porous Co (OH) 2/Ni (OH) 2 micro-rods with ultra-high specific surface area for energy storage. *Chem. Eng. J.* 428, 132123. doi:10.1016/j.cej.2021.132123